A note on rotational components of earthquake motions on ground surface for incident body waves

M. D. TRIFUNAC

Department of Civil Engineering, University of Southern California, Los Angeles, California 90007

This paper shows that the Fourier amplitude spectra of rocking and torsional components of strong shaking on ground surface can be derived exactly in terms of (1) wavelength of incident waves, (2) Fourier amplitude spectra of vertical (for incident P and SV waves) or horizontal (for incident SH waves) ground motion, and (3) the angle of incidence of plane body waves, θ_0. Application of these results in earthquake engineering is discussed.

INTRODUCTION

Rocking and torsional components of strong earthquake ground motion are beginning to attract the attention of engineering and research communities as it is becoming evident that those motions may contribute significantly to the overall response of structures to strong earthquake ground shaking[1-4]. With further development of strong motion instruments to record rotational components of strong motion[5], it will become possible to examine these experimentally. However, it may take a long time before sufficient data are gathered to facilitate reliable and detailed empirical studies. Therefore, in the interim, it is useful to explore the possibility of estimating them in terms of the corresponding translational components of strong motion, which have been recorded and studied more extensively.

The purpose of this paper is to show how the rocking and torsion of strong motion at ground surface associated with incident plane P, SV and SH waves can be determined exactly from the known translational components of ground motion there. Comparison of the torsional results presented here with those presented and reviewed by Nathan and MacKenzie[6] will show the nature of the previous approximate analyses.

Rotations of surface ground motion are derived by applying the curl operator on the vector components of displacements associated with incident waves. For incident body P, SV and SH waves, the corresponding surface displacements have been studied extensively and are available in classical literature on wave propagation[7,4]. It is noted, however, that many papers on this subject are either in error or incomplete. Typically, reflection of SV waves past the critical angle and the associated phase delays are rarely presented in detail. Such results are essential for interpretation of incident motion and serve as a basis for computing rotational components of strong shaking. Therefore, for completeness of this presentation, these classical results[7] are briefly summarized.

The aim of this note is to provide an analytical basis for estimation of rotational components of strong ground motion. To see how these can be used in engineering applications, one can study papers by Trifunac[8] and by Wong and Trifunac[9]. The first paper shows how different wave types can be associated with a train of waves

corresponding to strong ground shaking, and how through dispersion analysis for the site geology, one can determine the phase and group velocities for surface waves, the arrival times of body waves, and their relative contributions to the complete motion. The second paper shows how to construct artificial accelerograms empirically but using the physical nature of wave propagation as in Trifunac[8]. Finally, by using the results presented here in the superposition model employed by Wong and Trifunac[9], one can compute artificial accelerograms of ground rotations and their spectra.

INCIDENT P-WAVES

Figure 1 shows the coordinate system (x_1, x_2) and the incident and reflected rays associated with plane P wave reflecting off the free boundary of the elastic homogeneous and isotropic half-space $(x_2 \leqslant 0)$. Without loss of generality, it is assumed here that the incident and reflected rays are in the plane $x_3 = 0$. Particle motion amplitudes and their assumed positive directions in the planes perpendicular to the respective rays are then given by A_0, A_1 and A_2 where A_0 and A_1 are associated with incident and reflected P waves, while A_2 corresponds to the reflected SV wave. For this excitation and coordinate system, the only non-zero components of motion (at
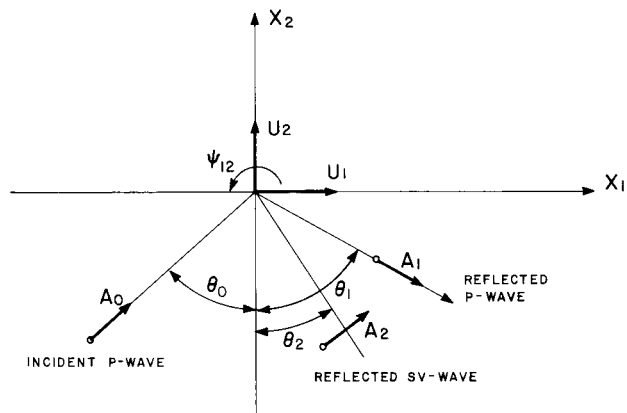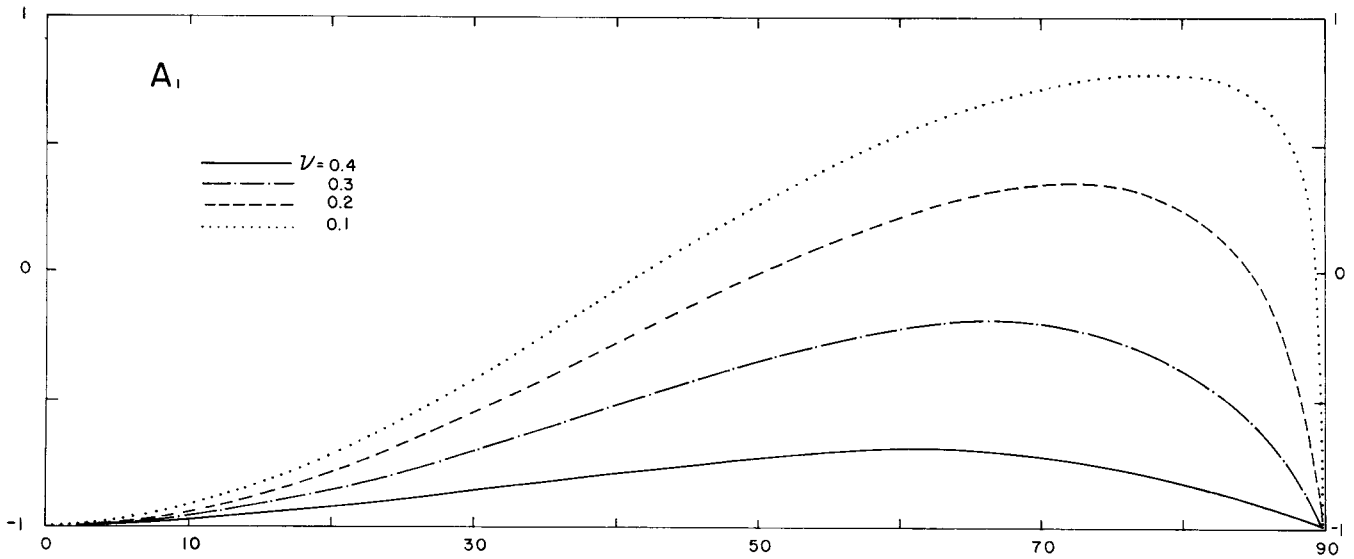

Figure 1. Coordinate system for incident p-wave

A₁

$\nu = 0.4$
            0.3
            0.2
            0.1

Figure 2. A_1-amplitude of reflected P-wave versus incidence angle θ_0 for $A_0 = 1$.

$x_2 = 0$) are

$$u_1 = (A_0 \sin \theta_0 + A_1 \sin \theta_1 + A_2 \cos \theta_2)\exp[i\kappa_0(x_1 \sin \theta_0 - c_L t)] \tag{1}$$

$$u_2 = (A_0 \cos \theta_0 - A_1 \cos \theta_1 + A_2 \sin \theta_2)\exp[i\kappa_0(x_1 \sin \theta_0 - c_L t)] \tag{2}$$

and

$$\psi_{12} = \tfrac{1}{2}\left(\frac{\partial u_2}{\partial x_1} - \frac{\partial u_2}{\partial x_2}\right) = \frac{i}{2} A_2 \kappa_2 \exp[i\kappa_0(x_1 \sin \theta_0 - c_L t)] \tag{3}$$

and u_1 and u_2 represent displacements in x_1 and x_2 directions while ψ_{12} represents rotation about x_3 axis. In equations (1), (2) and (3), κ_0 and κ_2 are given by

$$\kappa_0 = \frac{\omega}{c_L} \tag{4}$$

$$\kappa_2 = \frac{\omega}{c_T} \tag{5}$$

where ω is circular frequency and c_L and c_T represent velocities of P and SV waves. In the above equations t represents time and $i \equiv \sqrt{-1}$. It is seen that ψ_{12} is associated only with SV wave motion through A_2.

Since the wave length of SV waves is $\lambda = (2\pi/\omega)c_T$, ψ_{12} in equation (3) can be normalized as

$$\zeta_{12} = \frac{\psi_{12}}{\pi}\lambda \exp[-i\kappa_0(x_1 \sin \theta_0 - c_L t)] = A_2 \exp\left(i\frac{\pi}{2}\right) \tag{6}$$

It is seen that this normalized rotation associated with incident plane P with wave amplitude A_0 has amplitude A_2 and is phase-shifted relative to the incident motion by $\pi/2$.

The ampltiudes A_1 and A_2 are given by Achenbach[7],

$$\frac{A_1}{A_0} = \frac{\sin 2\theta_0 \sin 2\theta_2 - \kappa^2 \cos^2 2\theta_2}{\sin 2\theta_0 \sin 2\theta_2 + \kappa^2 \cos^2 2\theta_2} \tag{7}$$

and

$$\frac{A_2}{A_0} = \frac{2\kappa \sin 2\theta_0 \cos 2\theta_2}{\sin 2\theta_0 \sin 2\theta_2 + \kappa^2 \cos^2 2\theta_2} \tag{8}$$

with

$$\sin \theta_2 = \kappa^{-1} \sin \theta_0; \qquad \theta_1 = \theta_0$$

and

$$\kappa = \left[\frac{2(1-v)}{1-2v}\right]^{1/2} \tag{9}$$

where v is the Poisson's ratio.

Figures 2 and 3 show A_1 and A_2 versus θ_0 and for selected values of v. Figures 4, 5, 6a and 6b present the amplitudes of u_1, u_2, ξ_{12}/u_1 and ξ_{12}/u_2 versus θ_0 and for the same values of v.

INCIDENT *SV* WAVES

Figure 7 shows the coordinate system, ground motion amplitudes u_1 and u_2 and the ray directions with the assumed positive displacement amplitudes of incident (A_0) and reflected P (A_1) and SV (A_2) waves. For the incident ray of SV waves in $x = 0$ plane, the only non-zero components of motion are u_1, u_2 and ψ_{12}. For $\theta_0 < \sin^{-1}(1/\kappa)$, at $x_2 = 0$, these are given by

$$u_1 = (-A_0 \cos\theta_0 + A_1 \sin\theta_1 + A_2 \cos\theta_2)\exp[i\kappa_0(x_1 \sin\theta_0 - c_T t)] \tag{10}$$

$$u_2 = (A_0 \sin\theta_0 - A_1 \cos\theta_1 + A_2 \sin\theta_2)\exp[i\kappa_2(x_1 \sin\theta_0 - c_T t)] \tag{11}$$

and

$$\psi_{12} = \tfrac{1}{2}\left(\frac{\partial u_2}{\partial x_1} - \frac{\partial u_1}{\partial x_2}\right) = \frac{i\kappa_2}{2}(A_0 + A_2)\exp[i\kappa_0(x_1 \sin\theta_2 = c_T t)] \tag{12}$$

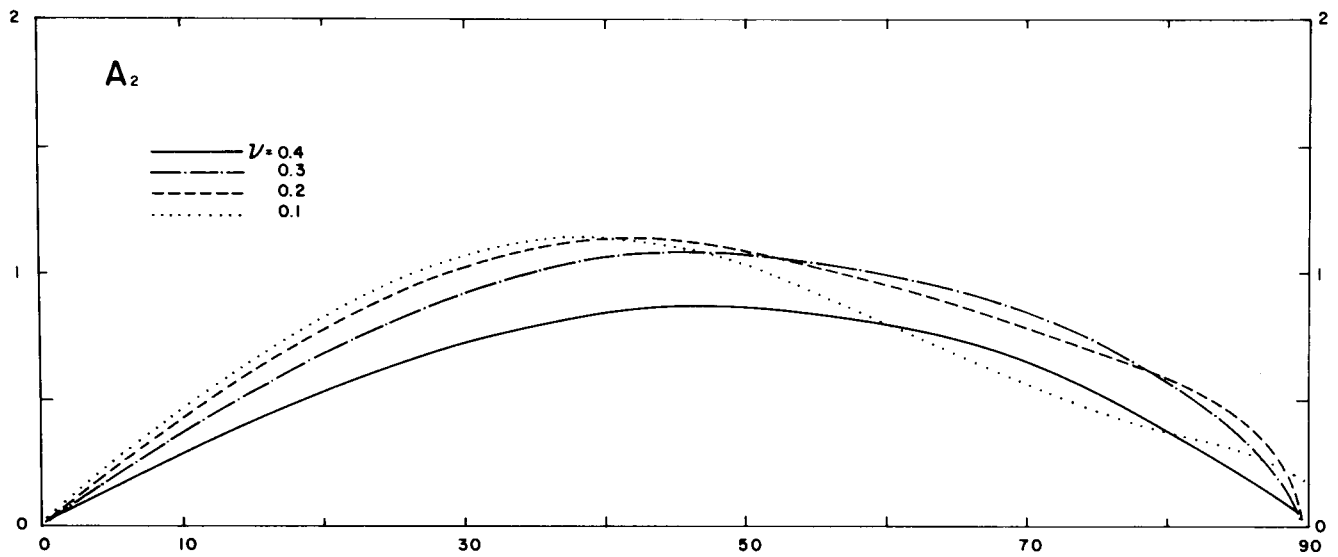*Figure 3. A_2-amplitude of reflected SV-wave versus incidence angle θ_0 for $A_0 = 1$.*
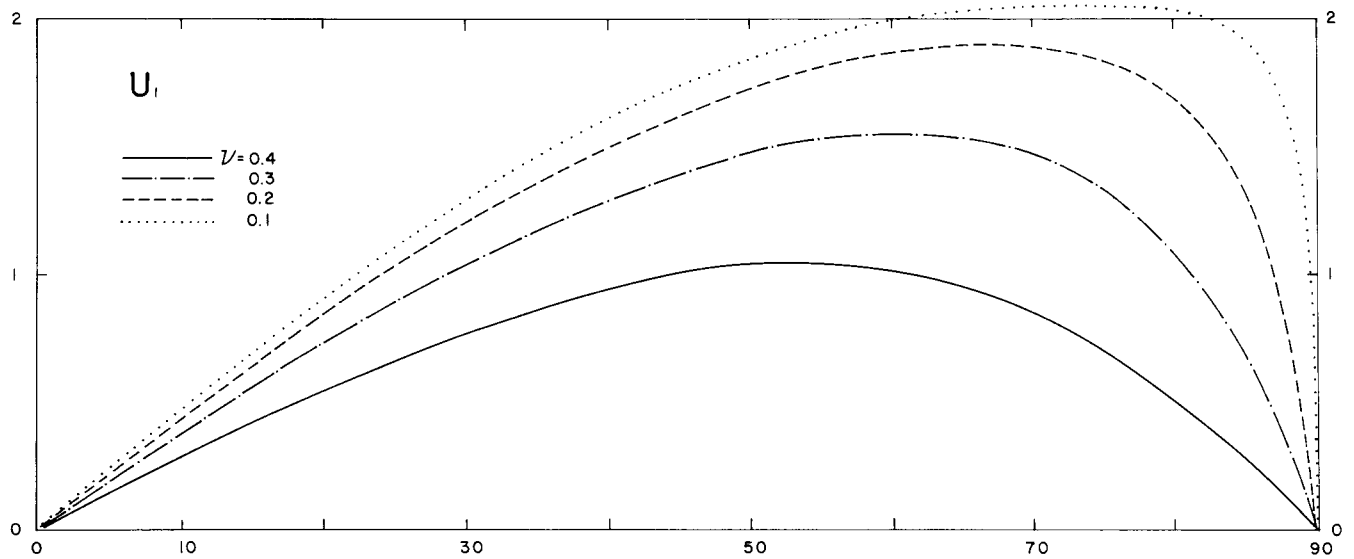

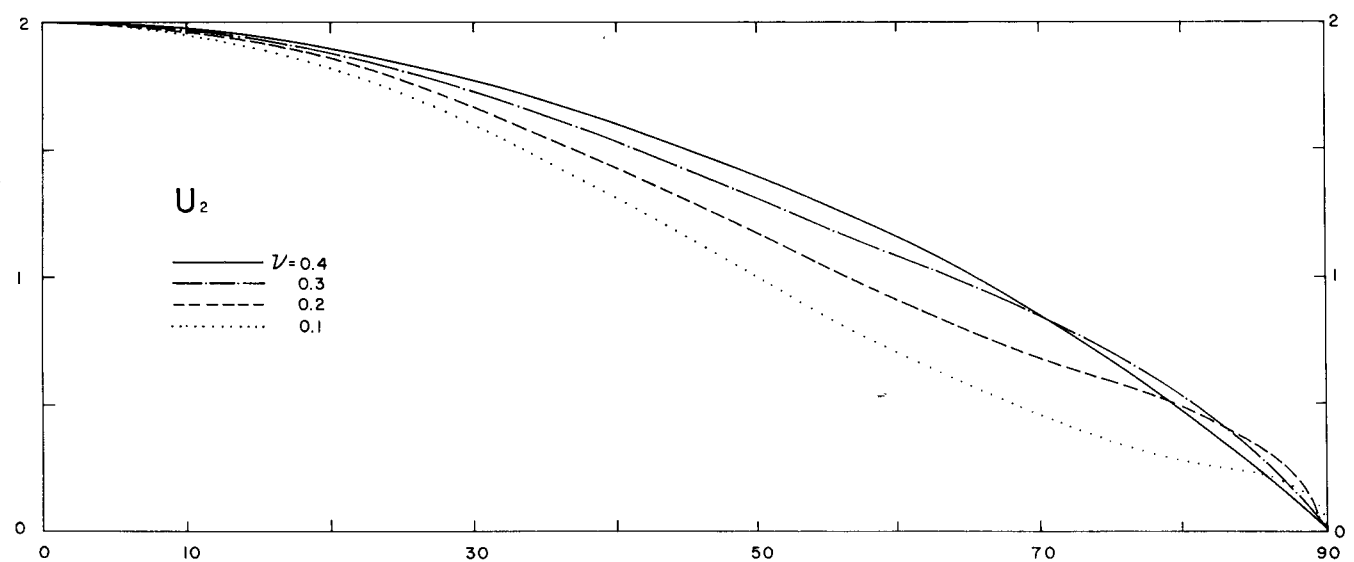*Figure 4. Horizontal displacement amplitude versus incidence angle θ_0 for $A_0 = 1$.*

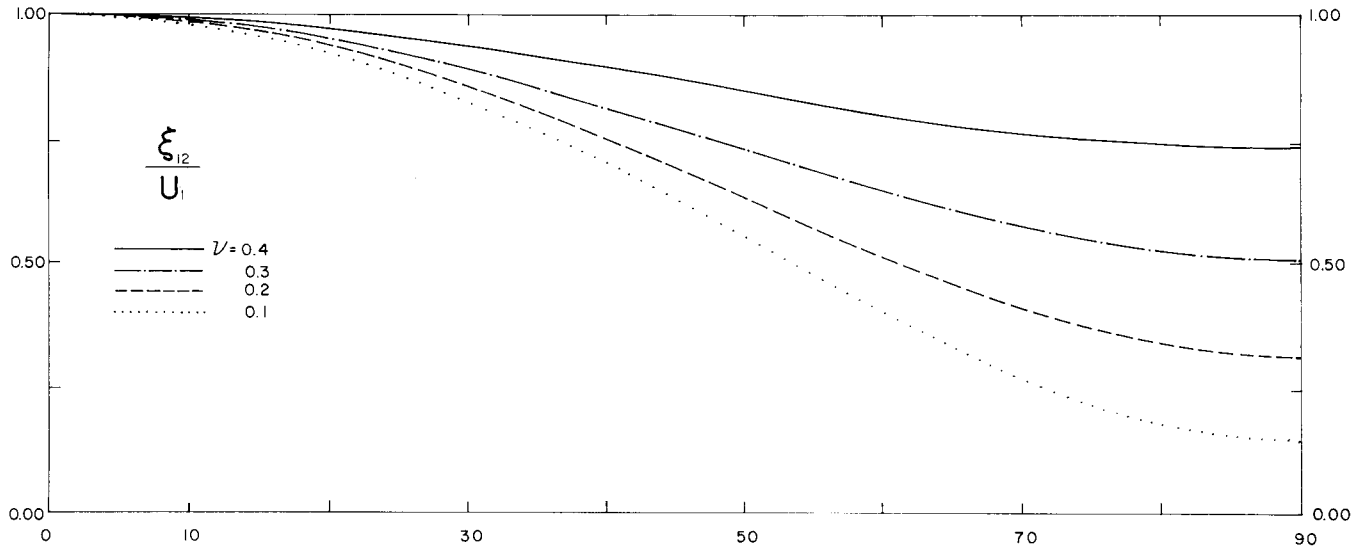*Figure 5. Vertical displacement amplitude versus incidence angle θ_0 for $A_0 = 1$.*

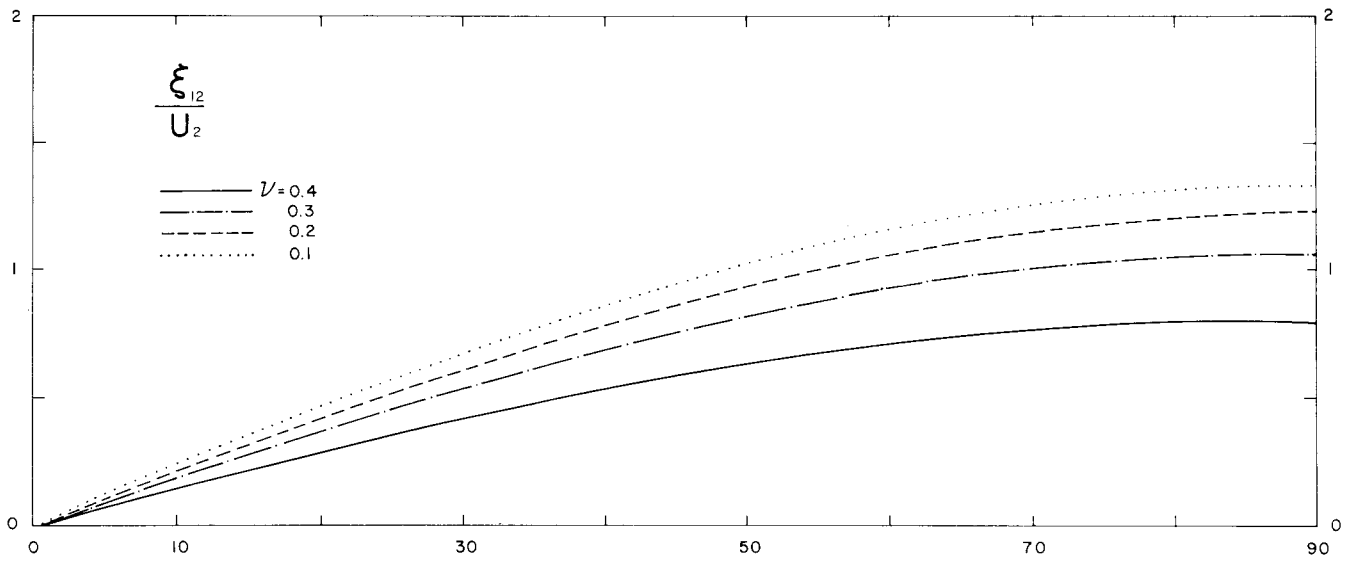Figure 6a. *Normalized rotation ζ_{12}/v_1 versus incidence angle θ_0.*

Figure 6b. *Normalized rotation ζ_{12}/v_2 versus incidence angle θ_0.*
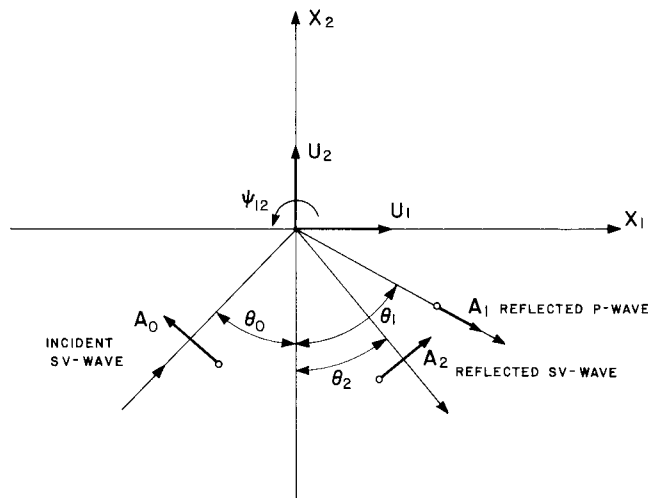
Figure 7. *Coordinate system for incident SV wave*

where[7]

$$\frac{A_1}{A_0} = \frac{-\kappa \sin 4\theta_0}{\sin 2\theta_0 \sin 2\theta_1 + \kappa^2 \cos^2 \theta_0} \qquad (13)$$

and

$$\frac{A_2}{A_0} = \frac{\sin 2\theta_0 \sin 2\theta_1 - \kappa^2 \cos^2 2\theta_0}{\sin 2\theta_0 \sin 2\theta_1 + \kappa^2 \cos^2 2\theta_0}. \qquad (14)$$

Using equation (5) and remembering that $\lambda = c_T 2\pi/\omega$ the normalized ψ_{12} for $\theta_0 < \sin^{-1}(1/\kappa)$ becomes

$$\xi_{12} = \frac{\psi_{12}\lambda}{\pi} \exp[-i\kappa_0(x_1 \sin \theta_0 - c_T t)] = (A_0$$

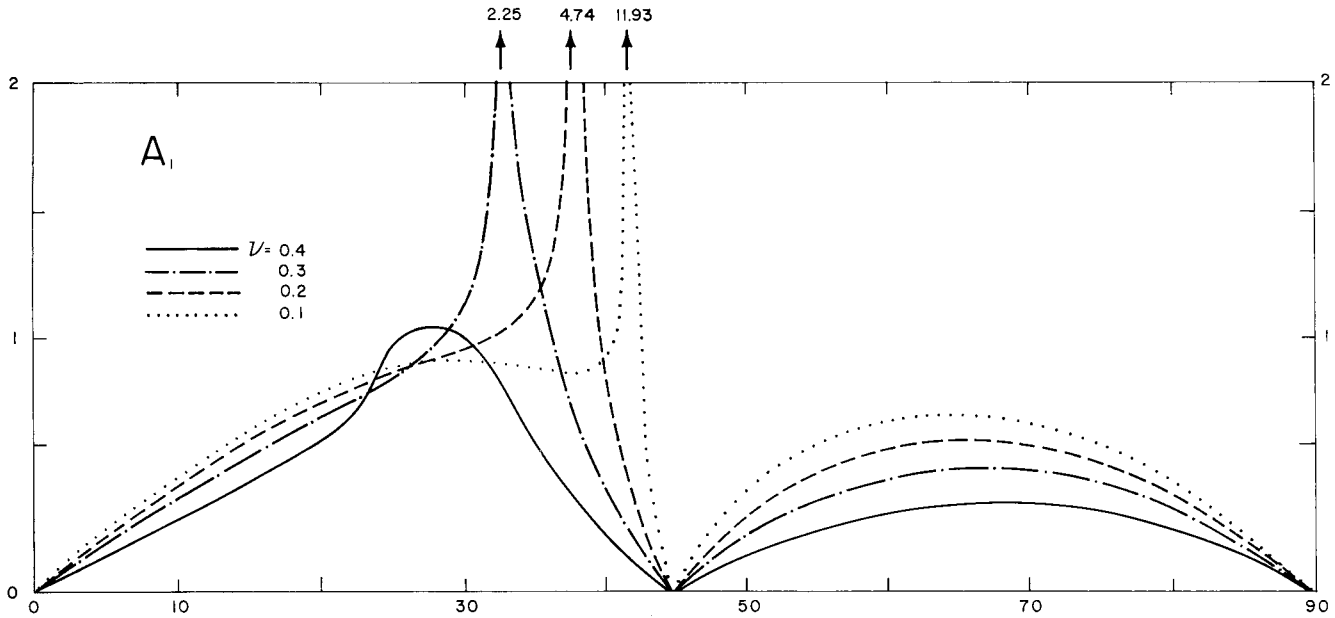$$+ A_2) \exp\left(i\frac{\pi}{2}\right). \qquad (15)$$

Figure 8. A_1-*amplitude of reflected P-wave versus incidence angle* θ_0, *for* $A_0 = 1$. A_1 *is real and negative for* $\theta_0 < \theta_{cr}$. *The modulus of* A_1 *is shown for* $\theta_0 > \theta_{cr}$.

For $\theta_0 = \sin^{-1}(1/\kappa) \equiv \theta_{cr}$, θ_1 becomes $\pi/2$, $A_1/A_0 = [4(\kappa^2 - 1)^{1/2}]/[\kappa(2 - \kappa^2)]$ and $A_2/A_0 = -1$. For $\theta_0 > \theta_{cr}$ components of motion at ground surface ($x_2 = 0$) become

$$u_1 = -A_0 \cos\theta_0 \exp[i\kappa_0(x_1 \sin\theta_0 - c_T t)]$$
$$+ S \sin\theta_1 \exp[i\kappa_0 \sin\theta_0(x_1 - c_L t/\kappa \sin\theta_0) - i\alpha]$$
$$- A_0 \cos\theta_2 \exp[i\kappa_0(x_1 \sin\theta_0 - c_T t) - 2i\alpha], \qquad (16)$$

and

$$u_2 = A_0 \sin\theta_0 \exp[i\kappa_0(x_1 \sin\theta_0 - c_T t)]$$
$$- S \cos\theta_1 \exp[i\kappa_0 \sin\theta_0(x_1 - c_L t/\kappa \sin\theta_0) - t\alpha]$$
$$- A_0 \sin\theta_2 \exp[i\kappa_0(x_1 \sin\theta_0 - c_T t) - 2i\alpha], \qquad (17)$$

and

$$\psi_{12} = \frac{i}{2}\kappa_2 A_0 [1 - \cos 2\alpha + i\sin 2\alpha]\exp[i\kappa_0(x_1 \sin \theta_0 - c_T t)] \qquad (18)$$

In equations (16) and (17)[7]

$$S = \frac{-A_0 \sin 4\theta_0}{[\kappa^2 \cos^4 2\theta_0 + 4(\kappa^2 \sin^2 \theta_0 - 1)\sin^2 2\theta_0 \sin^2 \theta_0]^{1/2}} \qquad (19)$$

with

$$\tan\alpha = \frac{2(\kappa^2 \sin^2 \theta_0 - 1)^{1/2} \sin 2\theta_0 \sin\theta_0}{\kappa \cos^2 2\theta_0}. \qquad (20)$$

and

$$|A_2/A_0| = 1 \qquad (21)$$

Normalizing equation (18) in the analogous to equation (13) there follows (for $x_2 = 0$)

$$\xi_{12} = \frac{\psi_{12}\lambda}{\pi}\exp[-i\kappa_0(x_1 \sin\theta_0 - c_T t)]$$
$$= A[\sin^2 2\alpha + (1 - \cos 2\alpha)^2]^{1/2}\exp(-i\varphi) \qquad (22)$$

where

$$\varphi = \tan^{-1}\frac{1 - \cos 2\alpha}{\sin 2\alpha} = \alpha. \qquad (23)$$

Figures 8 and 9 present A_1 and A_2 versus θ_0. Figures 10, 11, 12, 13 and 14 show $u_1, u_2, \xi_{12}, \alpha$ *and* $|\xi_{12}/u_1|$ for selected values of v.

INCIDENT *SH* WAVES

For incident *SH* waves, there is no mode conversion and hence there is only one reflected *SH* wave with $\theta_2 = \theta_0$ and $A_2 = A_0$ (Figure 15). The two non-zero components of motion are u_3 and ψ_{13}, which, in earthquake engineering use, corresponds to torsional ground motion. For these motions we have at $x_2 = 0$

$$u_3 = 2A_0 \exp[i\kappa_0(x_1 \sin\theta_0 - c_T t)] \qquad (24)$$

and

$$\psi_{13} = -\frac{1}{2}\frac{\partial u_3}{\partial x_1} = -A_0 i\kappa_0 \sin\theta_0 \exp[i\kappa_0(x_1 \sin \theta_0 - c_T t)] \qquad (25)$$

Normalizing ψ_{13} with respect to λ there follows

$$\xi_{13} = \frac{\psi_{13}\lambda}{\pi}\exp[-i\kappa_0(x_1 \sin\theta_0 - c_T t)] = -2A_0 \sin\theta_0 2^{-i(\pi/2)}. \qquad (26)$$
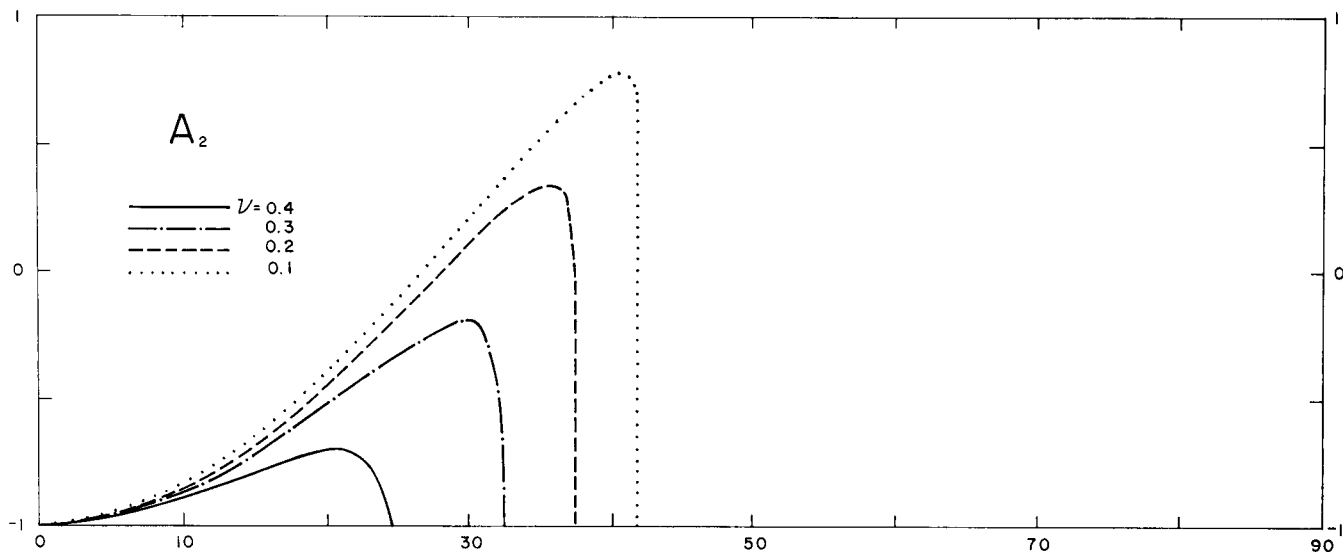
Figure 9. A_2-amplitude of reflected SV-wave versus incidence angle θ_0, for $A_0 = 1$. $A_2 = 0$ for $\theta_0 > \theta_{cr}$.

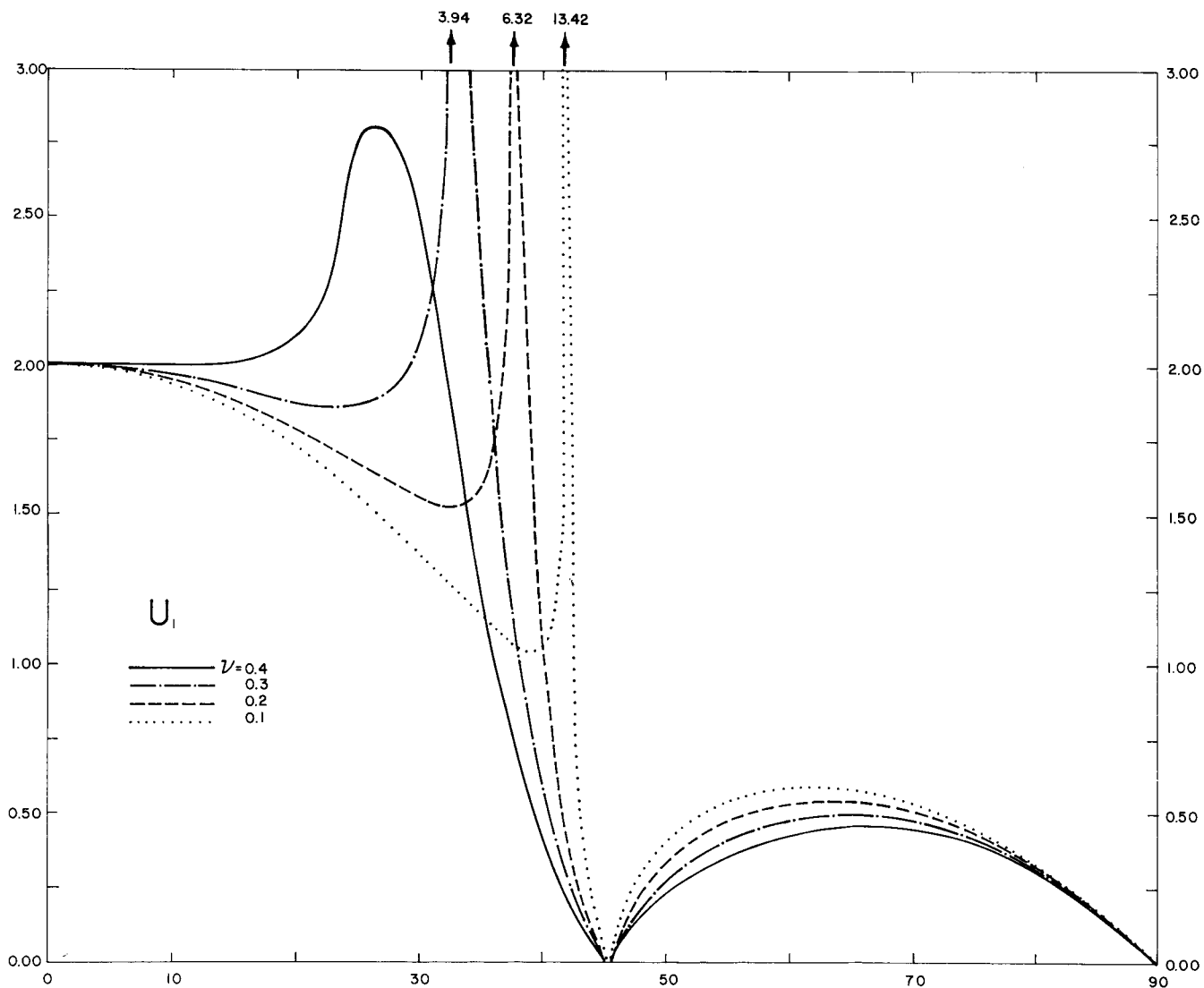*Figure 10. Horizontal displacement amplitude versus incidence angle θ_0 for $A_0 = 1$. U_1 is real and negative for $\theta_0 < \theta_{cr}$. The figure shows the modulus of U_1 for $\theta > \theta_{cr}$.*

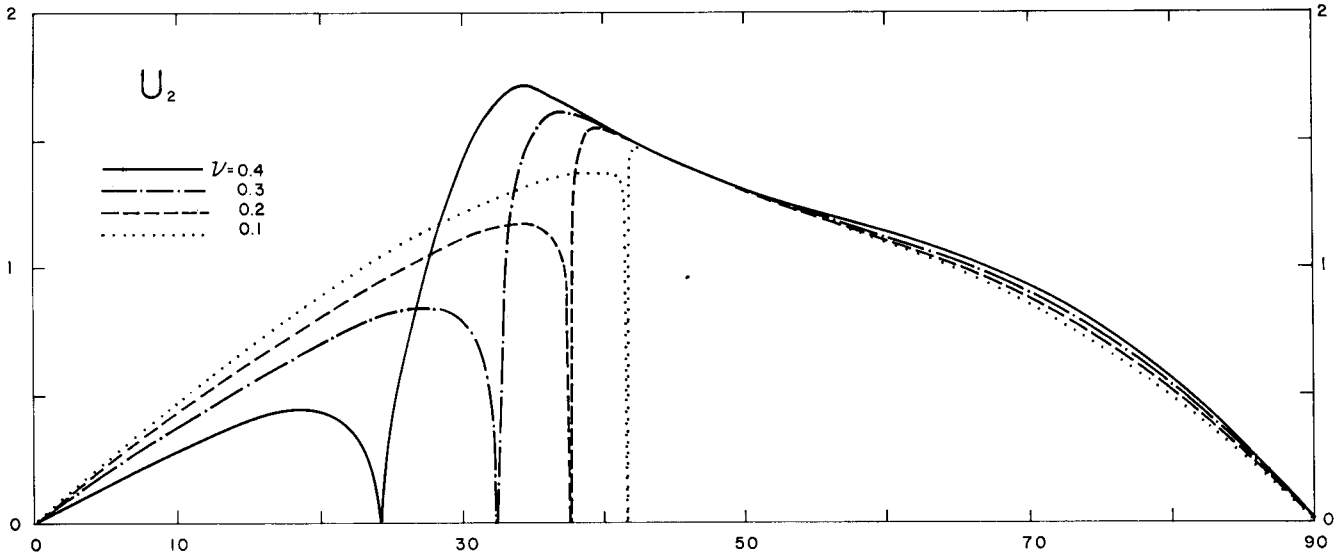*Figure 11. Vertical displacement amplitude versus incidence angle θ_0 for $A_0 = 1$. U_2 is real and positive for $\theta_0 < \theta_{cr}$. The figure shows the modulus of U_2 for $\theta > \theta_{cr}$. For $\theta_0 > \theta_{cr} |A_1| = s$.*
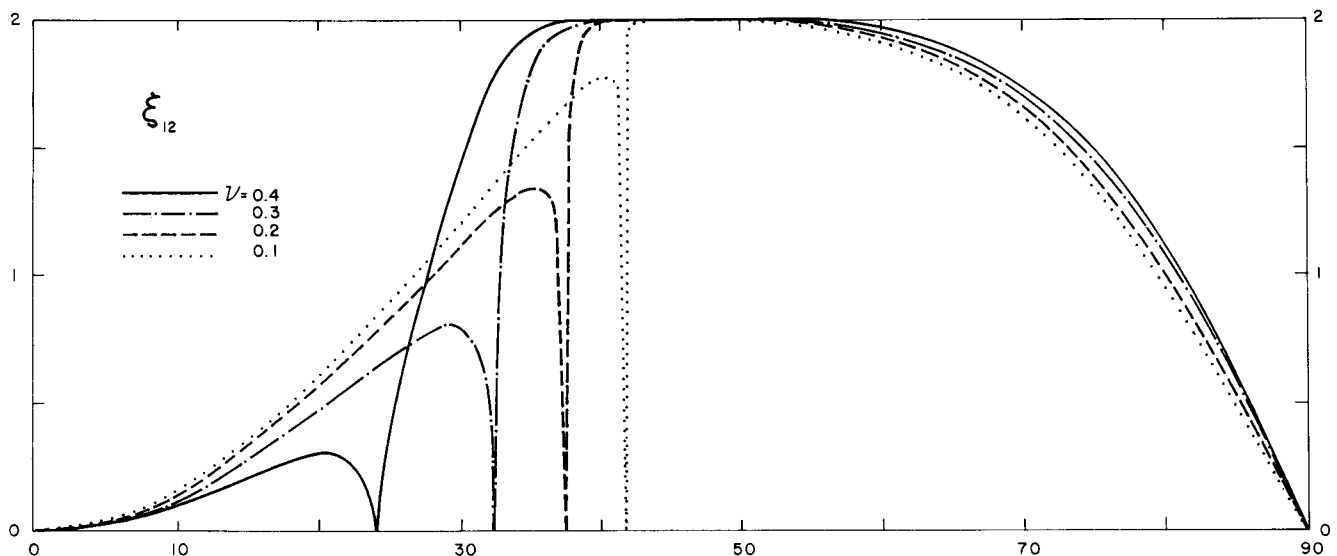

Figure 12. Normalized rotation amplitude ξ_{12} versus incidence angle θ_0.

DISCUSSION

From the preceding analysis, it is seen that the plane waves incident upon the free surface lead, in general, to three translational and three rotational components of ground motion. By conveniently rotating the coordinate system so that $x_3 = 0$ plane contains the incident and reflected rays it is easy to decouple these motions into those which result from (i) incident P and SV waves (u_1, u_2 and ψ_{12}) and (ii) incident SH waves (u_3 and ψ_{13}). Analysis of rotational components of ground motion at ground surface ($x_2 = 0$) further shows that the amplitudes of rocking (ψ_{12}) and torsion (ψ_{13}) increase linearly with frequency of motion ω.

Recording of the rotational components of strong ground motion is presently limited only to a small number of experimental programs[5], and it is likely that it will take many years before a significant body of such data becomes available for empirical and theoretical analyses. In the meantime, it is of interest to examine the possibility of estimating approximately the nature of the rotational

components of strong shaking by using the data on the amplitudes of translational motions and the knowledge of the types and the direction of approach of the incident waves. Since a common functional for description of strong earthquake ground motion is the Fourier amplitude spectrum, it is useful to examine the possibility of estimating Fourier spectra of rotations in terms of the Fourier amplitude spectra of horizontal or vertical motions. To this end, Figures 6a and 6b present the ratios of normalized rotations ξ_{12} and the amplitudes u_1 and u_2 for different angles of incident θ_0 for plane P wave. It can be shown that

$$\left| \frac{\xi_{12}}{u_1} \right| = \frac{1 - (2/\kappa^2)\sin^2 \theta_0}{(1 - 1/\kappa^2 \sin^2 \theta_0)^{1/2}} \tag{27}$$

and
$$\left| \frac{\xi_{12}}{u_2} \right| = \frac{2 \sin \theta_0}{\kappa} \tag{28}$$

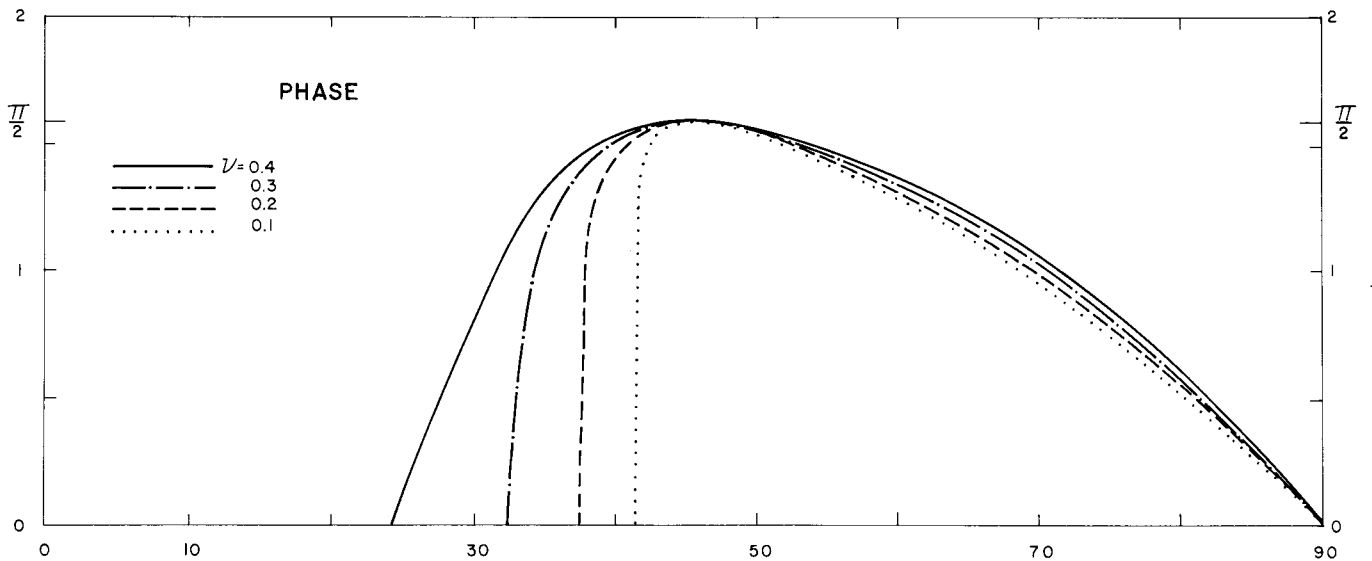where κ is given by equation (9).

PHASE

Figure 13.   PHASE versus incidence angle θ_0. It corresponds to (i) negative phase of A_1, (ii) one-half of negative phase of A_2, (iii) phase φ of ξ_{12}, (iv) $\pi/2$ minus the phase of U_2 for $\theta > \theta_{cr}$ and the phase of U_2 for $\theta < \theta_{cr}$, (v) π minus the phase of U_1 for $\theta_0 < 45°$ and the negative phase of U_1 for $\theta_0 > 45°$.

$$\left| \frac{\xi_{12}}{U_1} \right|$$
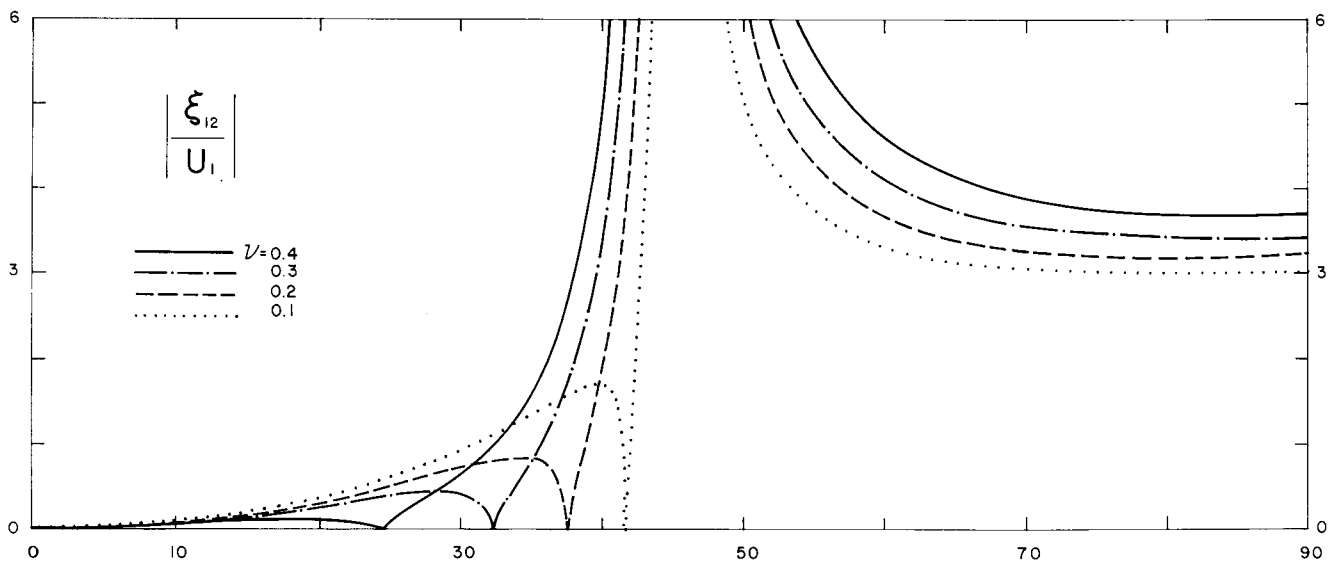
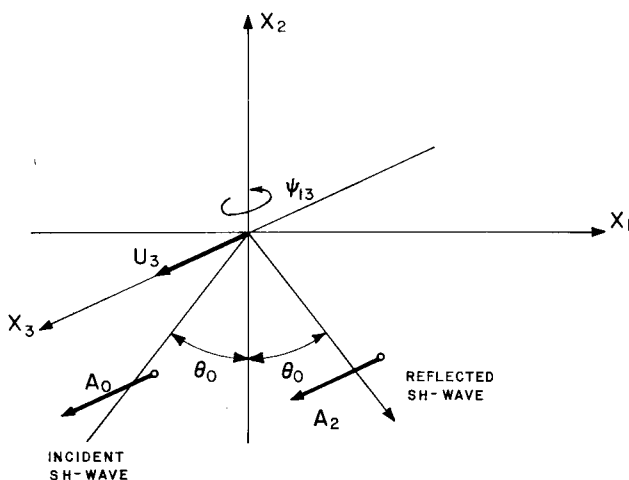*Figure 14.   Amplitude of $|\xi_{12}/U_1|$ versus incidence angle θ_0.*

Figure 15.   Coordinate system for incident SH-wave

As can be seen from Figures 6a and 6b and equations (27) and (28) both $|\xi_{12}/u_1|$ and $|\xi_{12}/u_2|$ change gradually with θ_0 so that either of the ratios can be used conveniently to estimate Fourier amplitude spectra of ψ_{12} for known Fourier amplitude spectra of vertical (u_2) or horizontal (u_1) ground motion resulting from incident P waves. The phase difference between ψ_{12} and u_1 or between ψ_{12} and u_2 is equal to $\pi/2$ as given by equations (1), (2) and (3).

Figure 14 presents the ratio of $|\xi_{12}/u_1|$ for incident SV waves and shows that its amplitudes blow up at $\theta_0 = 45°$ since $u_1 = 0$ there. This suggests that the rocking amplitudes of ground motion ψ_{12} for incident SV waves should not be estimated in terms of the Fourier amplitude spectra of the horizontal motion since the results would be too sensitive to the amplitudes of u_1 for θ_0 near 45°. In contrast the ratio $|\xi_{12}/u_2|$ can be shown to be

$$|\xi_{12}/u_2| = 2 \sin\theta_0 \qquad (29)$$

which is easy to use with Fourier amplitude spectra of u_2.

For incident SH waves, it is seen from equations (25) and (26) that

$$\left|\frac{\xi_{13}}{u_3}\right| = \sin\theta_0 \qquad (30)$$

with phase difference of $\pi/2$ between ξ_{12} and u_3.

CONCLUSIONS

The foregoing analysis shows that the Fourier amplitude spectra of rocking, ψ_{12}, and torsional, ψ_{13}, ground motion at the surface of homogeneous elastic and isotropic half-space can be written as

$$\psi_{1j} = A \frac{\pi}{\lambda} u_j \sin\theta_0 \qquad (31)$$

where λ is the wavelength of incident waves, u_j is the Fourier amplitude of vertical ($j=2$) or horizontal ($j=3$) ground motion, θ_0 is the incident angle (Figures 1, 7 and 15) and $A = 2/\kappa$ for incident P waves ($j=2$), $A = 2$ for incident SV waves ($j=2$), and $A = 1$ for incident SH waves ($j=3$).

Since the linear strong ground motion can be represented as a superposition of body waves at the surface of the elastic half-space, equation (31) can be employed to find exact Fourier amplitude spectra of rocking ψ_{12}, and torsion ψ_{13} associated with strong earthquake ground motion there. By Fourier synthesis, time function for ψ_{12} and ψ_{13} can also be derived assuming that the wave types leading to u_2, and their incidence angles θ_0, can be identified or assumed.

Finally, remembering that the phase velocity, c_x, in x_1 direction (see Figures 1, 7 and 15) is equal to $c/\sin\theta_0$ where c is the representative wave velocity (c_T for incident SV and SH waves and c_L for incident P waves) it is seen that

equation (31) can also be written as

$$\psi_{1j} = \frac{A}{2} \frac{\omega}{c_x} u_j. \qquad (32)$$

By employing this result in conjunction with the method for synthesis of artificial accelerograms[9], complete time history of rocking, ψ_{12}, and torsional, ψ_{13}, motions can be constructed.

REFERENCES

1 Kobori, T. and Shinozaki, Y. *Torsional vibration of structure due to obliquely incident SH waves*, 1975, Proc. Fifth World Conf. Earthquake Eng., 1, No. 22
2 Luco, J. E. Torsional Response of Structures for SH waves: The Case of Hemispherical Foundations, *Bull. Seism. Soc. Amer.*, 1976, **66**, 109–123
3 Bielak, J. Dynamic Response of Nonlinear Building–Foundation Systems, *Int. J. Earthquake Eng. and Struct. Dyn.*, 1978, **6**, 17–30
4 Lee, V. W. *Investigation of Three-Dimensional Soil–Structure Interaction*, 1979, Ph.D. Thesis, Dept. of Civil Engr., Report No. 79-11, U.S.C., Los Angeles
5 Shibata, H., Shigeta, T. and Sone, A. On Some Results of Observation of Torsional Ground Motions and Their Response Analysis, *Bull. Earthquake Resistant, Struct. Research Center*, 1976, **10**, 43–47
6 Nathan, N. D. and MacKenzie, J. R. Rotational Components of Earthquake Motion, *Canad J. of Civil Eng.*, 1975, **2**, 430–436
7 Achenbach, J. D. *Wave Propagation in Elastic Solids*, 1973, North-Holland/American Elsevier
8 Trifunac, M. D. Response Envelope Spectrum and Interpretation of Strong Earthquake Ground Motion, *Bull. Seism. Soc. Amer.*, 1971, **61**, 343–356
9 Wong, H. L. and Trifunac, M. D. Generation of Artificial Strong Motion Accelerograms, *Int. J. Earthquake Eng. and Struc. Dyn.*, 1979, 7, 509–527.